The [2:2] Site-Differentiated Clusters $[Fe_4S_4L_2(RNC)_6]$ Containing Two Low-Spin Iron(II) Sites

Christopher Goh, John A. Weigel, and R. H. Holm*

Department of Chemistry, Harvard University, Cambridge, Massachusetts 02138

Received April 27, 1994[⊗]

Whereas the chemistry of [1:3] site-differentiated Fe_4S_4 cubane-type clusters has been extensively explored, [2:2] clusters have not been similarly examined. A class of such clusters has been prepared and studied. Reaction of $[Fe_4S_4X_4]^{2-}$ (X = Cl^-, Br^-) with excess isonitrile in refluxing THF affords $[Fe_4S_4X_2(RNC)_6]$ (R = Me, *t*-Bu) in good yield. Substitution reactions readily occur at the halide sites to give $[Fe_4S_4L_2(t\text{-BuNC})_6]$ (L = RO^-, RS^-). Thiolate clusters can also be prepared by reaction of $[Fe_4S_4(SR)_4]^{2-}$ with excess RNC in the presence of Et_3NH^+. Mössbauer spectroscopy indicates the presence of two tetrahedral Fe(III) and two low-spin Fe(II) sites, which was confirmed by X-ray structural studies of two clusters. The compounds $[Fe_4S_4L_2(t\text{-BuNC})_6]$ (L = *p*-$MeC_6H_4O^-$ (**7**), PhS^- (**8**)) crystallize in monoclinic space group $P2_1/n$ with $Z = 4$. For **7**/**8**, a = 16.536(3)/21.900(6) Å, b = 12.133(2)/11.994(7) Å, c = 31.872(6)/22.865(7) Å, and β = 95.62(4)/101.69(2)°. The clusters closely approach idealized C_2 symmetry. Opposite faces of the $[Fe_4S_4]^{2+}$ cores contain two six-coordinate low-spin sites $Fe^{II}S_3(t\text{-BuNC})_3$ and two tetrahedral sites $Fe^{III}S_2L_2$. The low-spin sites are isolated from each other by 3.46 Å and are separated from the tetrahedral sites by 3.0−3.1 Å. The two tetrahedral sites are separated by Fe−Fe distances of 2.766(2) Å (**7**) and 2.730(4) Å (**8**) and are implicated in antiferromagnetically coupled $[Fe_2S_2]^{2+}$ fragments. Core structures of three [2:2] clusters are essentially congruent, thereby defining the structural motif for $[Fe_4S_4]^{2+}$ clusters containing two tetrahedral Fe(III) and two low-spin six-coordinate Fe(II) sites. The redox characteristics of the clusters are reported. The set $[Fe_4S_4L_2(RNC)_6]$ (L = halide, RO^-, RS^-) comprises the largest and most thoroughly characterized class of [2:2] site-differentiated clusters.

Introduction

The tendency of the anionic mixed-ligand cubane-type clusters $[Fe_4S_4L_{4-n}L'_n]^{2-}$ (n = 1−3) to exist in disproportionation equilibria in polar solvents has led to the development in this laboratory of iron [1:3] site-differentiated clusters of the types $[Fe_4S_4(LS_3)L']^{z-}$ [1-4] and $[Fe_4S_4(c\text{-}LS_3)L']^{z-}$.[5] These clusters are derived from large semirigid trithiolate ligands which bind the $[Fe_4S_4]^{2+}$ core at three of the four iron sites. They are immune to disproportionation and offer the considerable advantage of regiospecific substitution at the unique iron atom.[1-6] More recently, we prepared a single example of an iron [2:2] site-differentiated cluster involving the binding of isonitriles.[7] This class of clusters is elaborated in the present work. Pertinent reactions and relevant clusters **1**−**15** are set out in Figure 1.

Given earlier indications that isonitriles can displace chloride or acetate from $[Fe_4S_4]^{2+}$ clusters,[8] we have demonstrated the occurrence of the equilibrium reaction (1).[7,9] Site-differentiated

$$[Fe_4S_4(LS_3)Cl]^{2-} + 3RNC \rightleftarrows [Fe_4S_4(LS_3)(RNC)_3]^- + Cl^- \quad (1)$$

cluster **1** contains the electronically delocalized $[Fe_4S_4]^{2+}$ core with an $S = 0$ ground state. Reaction product **2** (R = *t*-Bu) was isolated and was shown to contain at the unique subsite a low-spin six-coordinate Fe(II) atom that is bound to a cuboidal $[Fe_3S_4(SR)_3]^{3-}$ fragment with spin $S = 2$.[7,9] This was the first instance of a spin-isolated $[Fe_3S_4]^0$ fragment outside a protein environment.[10] Further work afforded one instance of reaction 2, which yielded a neutral cluster stable in solvents of low

$$[Fe_4S_4Cl_4]^{2-} + 6t\text{-BuNC} \rightleftarrows [Fe_4S_4Cl_2(t\text{-BuNC})_6] + 2Cl^- \quad (2)$$

polarity. The X-ray structure and Mössbauer spectrum of this molecule confirmed the existence of low-spin $Fe^{II}S_3(RNC)_3$ sites; from comparative properties a structurally congruent site must be present in $[Fe_4S_4(LS_3)(RNC)_3]^-$. $[Fe_4S_4Cl_2(t\text{-BuNC})_2]$ is a [2:2] site-differentiated cluster; in this sense it resembles the neutral clusters $[Fe_4S_4X_2L_2]$ (X = I^-, RS^-; L = $SPPh_3$, $SC(NHR)_2$) prepared by Pohl and co-workers.[11] Its site-specific reactivity and the scope of formation of similar clusters have not been previously established. These issues have been addressed in the present investigation, which represents continuing development[12] in this laboratory of the chemistry of site-differentated Fe_4S_4 clusters.

[⊗] Abstract published in *Advance ACS Abstracts,* September 15, 1994.

(1) Holm, R. H.; Ciurli, S.; Weigel, J. A. *Prog. Inorg. Chem.* **1990**, *38*, 1. LS_3 = trianion of 1,3,5-tris((4,6-dimethyl-3-mercaptophenyl)thio)-2,4,6-tris(*p*-tolylthio)benzene.
(2) Stack, T. D. P.; Holm, R. H. *J. Am. Chem. Soc.* **1988**, *110*, 2484.
(3) Ciurli, S.; Carrié, M.; Weigel, J. A.; Carney, M. J.; Stack, T. D. P.; Papaefthymiou, G. C.; Holm, R. H. *J. Am. Chem. Soc.* **1990**, *112*, 2654.
(4) Stack, T. D. P.; Weigel, J. A.; Holm, R. H. *Inorg. Chem.* **1990**, *29*, 3745.
(5) Whitener, M. A.; Peng, G.; Holm, R. H. *Inorg. Chem.* **1990**, *30*, 2411. c-LS_3 is a macrocyclic polyether trithiolate(3−).
(6) Weigel, J. A.; Holm, R. H. *J. Am. Chem. Soc.* **1991**, *113*, 4184.
(7) Weigel, J. A.; Srivastava, K. K. P.; Day, E. P.; Münck, E.; Holm, R. H. *J. Am. Chem. Soc.* **1990**, *112*, 8015.
(8) Johnson, R. W.; Holm, R. H. *J. Am. Chem. Soc.* **1978**, *100*, 5338.
(9) Weigel, J. A.; Holm, R. H.; Surerus, K. K.; Münck, E. *J. Am. Chem. Soc.* **1989**, *111*, 9246.
(10) Holm, R. H. *Adv. Inorg. Chem.* **1992**, *38*, 1 and references therein.
(11) (a) Saak, W.; Pohl, S. *Z. Naturforsch.* **1988**, *43B*, 813. (b) Pohl, S.; Bierbach, U. *Z. Naturforsch.* **1991**, *46B*, 68. (c) Bierbach, U.; Saak, W.; Pohl, S.; Haase, D. *Z. Naturforsch.* **1991**, *46B*, 1629. (d) Pohl, S.; Bierbach, U. *Z. Naturforsch.* **1992**, *47B*, 1266.
(12) Cai, L.; Weigel, J. A.; Holm, R. H. *J. Am. Chem. Soc.* **1993**, *115*, 9289.

0020-1669/94/1333-4861$04.50/0

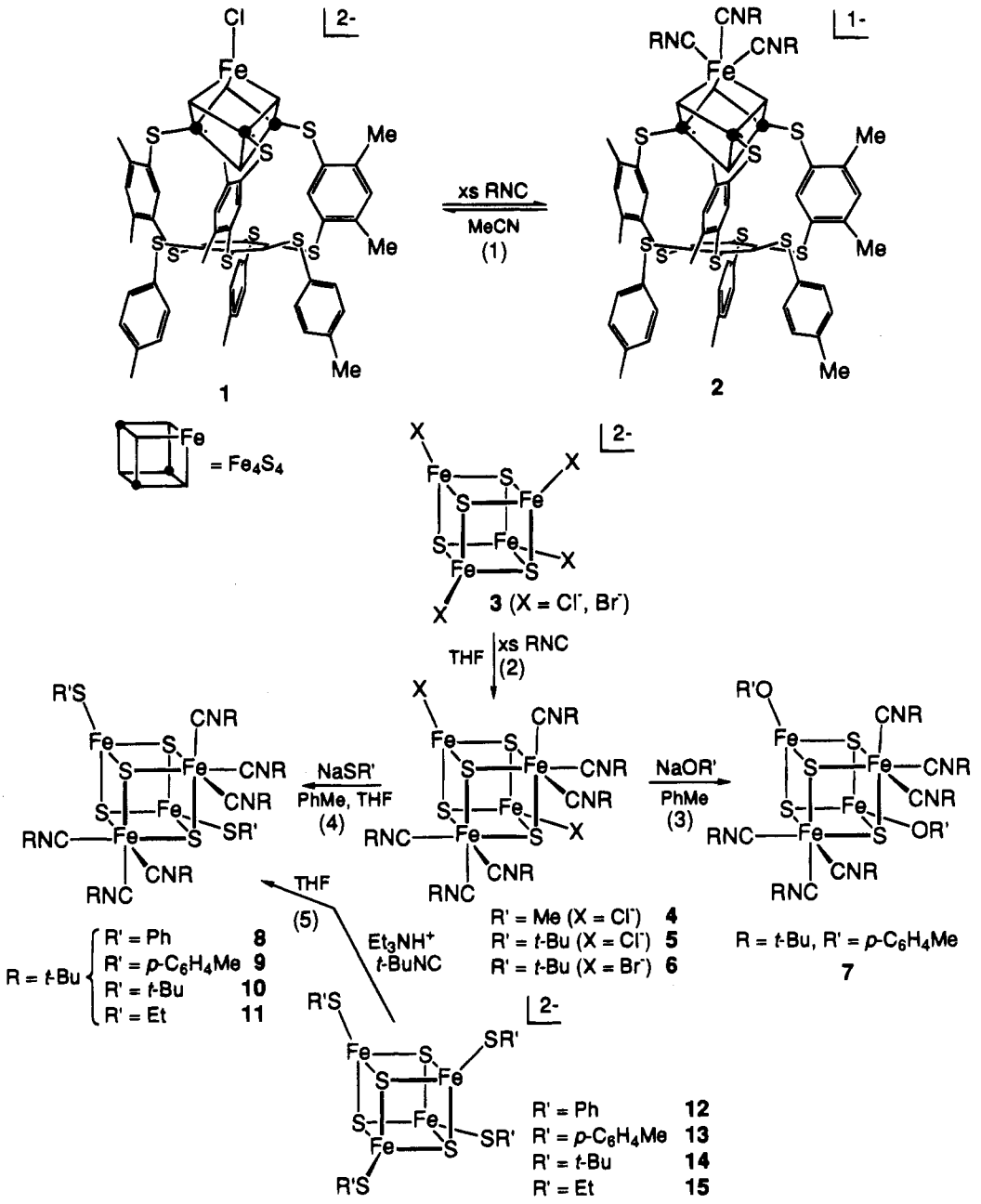

Figure 1. Schematic depiction of the synthesis and structures of site-differentiated tris(isonitrile) Fe_4S_4 clusters including the [1:3] cluster **2**[7,9] and the [2:2] clusters **4**–**11**. Thiolate-substituted clusters **8**–**11** have been prepared by two different methods (reactions 4 and 5). Precursor clusters **12**–**15** for reaction 5 are also shown.

Experimental Section

Preparation of Compounds. All operations were performed under anaerobic conditions. Solvents were freshly degassed prior to use. The steps of volume reduction and drying were performed in vacuo. *Note*: Several of the preparations below utilize $(Et_3NH)(ClO_4)$; while in our experience this compound is stable, due care with regard to a potential explosive hazard should be exercised in its use.

$[Fe_4S_4Cl_2(MeNC)_6]$. To a black suspension of 4.63 g (3.95 mmol) of $(Ph_4P)_2[Fe_4S_4Cl_4]$[13] in 200 mL of THF was added with stirring 4.29 mL (79 mmol) of MeNC.[14] The mixture was stirred for 2 d, during which the color of the suspended solid changed from green-black to blue-purple. The clear supernatant was removed, and the solid residue was washed with 3 × 25 mL of acetonitrile (to remove Ph_4PCl) and then with ether. After being dried, the product was obtained as 1.72 g (65%) of blue-purple solid. An analytical sample was recrystallized from DMF/ether. Absorption spectrum (DMF): λ_{max} (ϵ_M) 267 (sh, 13 900), 530 (2050) nm. IR (KBr): ν_{NC} 2188, 2167 cm^{-1}. ^1H NMR (Me_2SO-d_6): δ 0.95 (2), −0.64 (1). Anal. Calcd for $C_{12}H_{18}Cl_2Fe_4N_6S_4$: C, 21.57; H, 2.71; Cl, 10.60; Fe, 33.40; N, 12.56; S, 19.18. Found: C, 21.60; H, 2.82; Cl, 10.74; Fe, 33.31; N, 12.42; S, 19.02.

$[Fe_4S_4Br_2(t\text{-}BuNC)_6]$. To a black suspension of 330 mg (0.35 mmol) of $(Et_4N)_2[Fe_4S_4Br_4]$[13] in 50 mL of THF was added 796 μL (7.1 mmol) of *t*-BuNC,[15] causing an immediate color change to brown-purple and dissolution of the solid. The solution was refluxed for 1 h, cooled to room temperature, and filtered through a Celite plug. Addition of 50 mL of ether to the filtrate and storage overnight at −20 °C followed by filtration afforded 210 mg (60%) of product as a black-purple crystalline solid. An analytical sample was prepared by crystallization from THF/ether. Absorption spectrum (CH_2Cl_2): λ_{max} (ϵ_M) 289 (sh, 26 200), 354 (sh, 7290), 403 (sh, 3980), 481 (3200), 538 (3300) nm.

(13) Wong, G. B.; Bobrik, M. A.; Holm, R. H. *Inorg. Chem.* **1978**, *17*, 578.
(14) Casanova, J., Jr.; Schuster, R. E.; Werner, N. D. *J. Chem. Soc.* **1963**, 4280.
(15) Weber, W. P.; Gokel, G. W.; Ugi, I. K. *Angew. Chem., Int. Ed. Engl.* **1972**, *11*, 530.

IR (KBr): ν_{NC} 2141, 2118 cm^{-1}. ^1H NMR spectrum (MeCN): δ 1.56 (1), 1.41 (2). Anal. Calcd for $C_{30}H_{54}Br_2Fe_4N_6S_4$: C, 35.67; H, 5.39; Br, 15.82; Fe, 22.11; N, 8.32. Found: C, 35.78; H, 5.34; Br, 15.76; Fe, 22.21; N, 8.24.

$[Fe_4S_4(O\text{-}p\text{-}tol)_2(t\text{-}BuNC)_6]$. To a suspension of 300 mg (0.33 mmol) of $[Fe_4S_4Cl_2(t\text{-}BuNC)_6]$[7] in 20 mL of toluene was added with stirring 370 μL (3.3 mmol) of *t*-BuNC, followed by 93 mg (0.72 mmol) of solid Na(O-*p*-C_6H_4Me). The mixture was stirred overnight, during which a gradual color change from dark purple to orange-brown occurred, and was filtered through a Celite plug. The filtrate was treated with 10 mL of hexanes, and the mixture was maintained at −20 °C overnight. The solid was collected by filtration, washed with hexanes, and dried to afford 290 mg (84%) of product as brown needles. An analytical sample was recrystallized from toluene/hexane. Absorption spectrum (CH_2Cl_2): λ_{max} (ϵ_M) 330 (sh, 14 800), 431 (10 800), 502 (sh, 8200). IR (KBr): ν_{NC} 2141, 2113 cm^{-1}. ^1H NMR spectrum (MeCN): δ 0.48 (*o*-H), 1.28 (2, *t*-Bu), 1.68 (1, *t*-Bu), 8.61 (*p*-Me), 12.27 (*m*-H). Anal. Calcd for $C_{44}H_{68}Fe_4N_6O_2S_4$: C, 49.64; H, 6.44; Fe, 20.90; N, 7.89; S, 12.05. Found: C, 49.28; H, 6.39; Fe, 21.38; N, 7.82; S, 13.37.

$[Fe_4S_4(SPh)_2(t\text{-}BuNC)_6]$. Method A. To a suspension of 500 mg (0.54 mmol) of $[Fe_4S_4Cl_2(t\text{-}BuNC)_6]$ in 50 mL of toluene was added with stirring 610 μL (5.40 mmol) of *t*-BuNC, followed by 170 mg (1.4 mmol) of solid NaSPh. The mixture was stirred overnight, during which a gradual color change from dark purple to deep burgundy was observed. To the filtrate resulting from filtration of the mixture through a Celite plug was added an equal volume of hexanes, and the solution was stored overnight at −20 °C. The solid was collected by filtration, washed with hexanes, and dried to give 260 mg (45%) of product as dark brown platelets. Absorption spectrum (CH_2Cl_2): λ_{max} (ϵ_M) 290 (sh, 22 600), 461 (6120) nm. IR (KBr): ν_{NC} 2146, 2123 cm^{-1}. ^1H NMR spectrum (MeCN): δ 1.35 (2, *t*-Bu), 1.59 (1, *t*-Bu), 2.43 (*p*-H), 3.50 (*o*-H), 10.49 (*m*-H). This compound was not analyzed; its identity was established by NMR and an X-ray structural determination.

Method B. To a stirred solution of 582 mg (0.397 mmol) of $(Ph_4P)_2[Fe_4S_4(SPh)_4]$[16] and 669 μL (5.96 mmol) of *t*-BuNC in 50 mL of acetonitrile was slowly added a solution of 308 mg (731 mmol) of $(Et_3NH)(BPh_4)$[17] in 5 mL of acetonitrile. The reaction mixture was stirred for 15 min, during which the color changed from brown to burgundy-brown and a white solid precipitated. The mixture was filtered, the solvent was removed, and the solid residue was dissolved in THF. The solution was separated from undissolved materials by filtration through a Celite plug, and the volume of the filtrate was reduced to *ca.* 10 mL. An equal volume of hexanes was added. The solution was stored overnight at −20 °C and filtered to afford 277 mg (68%) of brown crystalline product, identical in all respects with the product of method A.

$[Fe_4S_4(S\text{-}p\text{-}tol)_2(t\text{-}BuNC)_6]$. To a stirred solution of 930 mg (0.842 mmol) of $(Et_4N)_2[Fe_4S_4(S\text{-}p\text{-}tol)_4]$[16] and 1.89 mL (16.8 mmol) of *t*-BuNC was slowly added a solution of 341 mg (1.69 mmol) of $(Et_3NH)(ClO_4)$ in 5 mL of acetonitrile. The reaction mixture was stirred for 1 h, during which a gradual color change from dark olive-green to burgundy-brown was observed. The solvent was removed, the solid residue was dissolved in ether, and the mixture was filtered. The volume of the filtrate was reduced to 20 mL, and the solution was stored at −60 °C for 24 h. The product was collected by filtration as 670 mg (73%) of a brown crystalline solid. An analytical sample was obtained by recrystallization from ether at −20 °C. Absorption spectrum (CH_2Cl_2): λ_{ax} (ϵ_M) 255 (sh, 44 200), 336 (sh, 16 600), 468 (sh, 9660), 493 (9860) nm. IR (KBr): ν_{NC} 2142, 2116 cm^{-1}. ^1H NMR (MeCN): δ 1.36 (2, *t*-Bu), 1.60 (1, *t*-Bu), 3.40 (*o*-H), 7.02 (*p*-Me), 10.36 (*m*-H). Anal. Calcd for $C_{44}H_{68}Fe_4N_6S_6$: C, 48.18; H, 6.25; Fe, 20.37; N, 7.66; S, 17.54. Found: C, 48.09; H, 6.19; Fe, 20.45; N, 7.70; S, 17.51.

$[Fe_4S_4(S\text{-}t\text{-}Bu)_2(t\text{-}BuNC)_6]$. Method A. To a purple solution of 603 mg (0.65 mmol) of $[Fe_4S_4Cl_2(t\text{-}BuNC)_6]$ in 100 mL of THF was added with stirring 1.10 mL (9.8 mmol) of *t*-BuNC, followed by a solution of 1.44 mmol of LiS-*t*-Bu (from equimolar *t*-BuSH and $LiEt_3BH$) in 20 mL of THF. The color of the solution turned rapidly to brown. Solvent was removed, leaving a brown residue, which was dissolved in toluene. This solution was filtered through a Celite plug. The filtrate was layered with 4 times the volume of hexanes and stored at −20 °C overnight. The solid material was collected by filtration, washed thoroughly with hexanes, and dried to afford the product as 428 mg (64%) of brown microcrystalline solid. An analytical sample was recrystallized from ether at −20 ° C. Absorption spectrum (CH_2Cl_2): λ_{max} (ϵ_M) 319 (sh, 19 900), 445 (10 800), 491 (sh, 8890), 566 (sh, 4060) nm. IR (KBr): ν_{CN} 2139, 2114 cm^{-1}. ^1H NMR (MeCN): δ 1.39 (2, *t*-BuNC), 1.58 (1, *t*-BuNC), 5.20 (S-*t*-Bu). Anal. Calcd for $C_{38}H_{72}Fe_4N_6S_6$: C, 44.36; H, 7.05; Fe, 21.71; N, 8.17; S, 18.70. Found: C, 44.40; H, 7.02; Fe, 21.61; N, 8.25; S, 18.66.

Method B. To a stirred solution of 690 mg (712 mmol) of $(Et_4N)_2[Fe_4S_4(S\text{-}t\text{-}Bu)_4]$[16] and 1.60 mL (14.2 mmol) of *t*-BuNC in 50 mL of acetonitrile was slowly added with stirring a solution of 287 mg (1.42 mmol) of $(Et_3NH)(ClO_4)$ in 10 mL of acetonitrile. An immediate color change from dark olive-green to orange-brown was observed. The mixture was stirred for 2 h, and the solvent was removed. The solid brown residue was dissolved in 40 mL of ether, and the solution was filtered. The filtrate was maintained at −20 °C overnight and filtered to yield 450 mg (61%) of a brown crystalline solid, obtained in analytical purity and identical in all respects with the product of method A.

$[Fe_4S_4(SEt)_2(t\text{-}BuNC)_6]$. Method A. To a purple solution of 302 mg (0.328 mmol) of $[Fe_4S_4Cl_2(t\text{-}BuNC)_6]$ in 50 mL of THF was added with stirring 56 mg (0.66 mmol) of solid NaSEt. Over the first 5 min, there was a gradual color change to brown. The reaction mixture was stirred overnight and filtered to remove a white solid. The volume of the filtrate was reduced in vacuo to *ca.* 10 mL, and 30 mL of hexane was layered onto the solution. The mixture was stored at −20 °C for 5 d and filtered. The product was obtained as 210 mg (66%) of a brown solid. An analytical sample was recrystallized from benzene/pentane. Absorption spectrum (CH_2Cl_2): λ_{max} (ϵ_M) 320 (sh, 18 600), 438 (10 200), 494 (sh, 8130), 562 (sh, 4540) nm. IR (KBr): ν_{NC} 2141, 2117 cm^{-1}. ^1H NMR spectrum (MeCN): δ 1.38 (2, *t*-Bu), 1.59 (1, *t*-Bu), 4.49 (CH_3), 34.4 (CH_2). Anal. Calcd for $C_{34}H_{64}Fe_4N_6S_6$: C, 41.99; H, 6.63; Fe, 22.97; N, 8.64; S, 19.78. Found: C, 41.78; H, 6.51; Fe, 23.10; N, 8.58; S, 19.88.

Method B. To a stirred solution of 510 mg (0.400 mmol) of $(Ph_4P)_2[Fe_4S_4(SEt)_4]$[16] and 0.700 mL (6.20 mmol) of *t*-BuNC in 100 mL of THF was slowly added a solution of 161 mg (0.800 mmol) of $(Et_3NH)(ClO_4)$ in 3.6 mL of acetonitrile. The reaction mixture was stirred for 1 h, during which a gradual color change from dark olive-green to orange-brown was observed. The solvent was removed, the solid brown residue was dissolved in benzene, and the solution was filtered to remove some insoluble material. Removal of solvent and drying afforded the product as 320 mg (83%) of a brown solid, identical in all respects with the product of method A.

Collection and Reduction of X-ray Data. Diffraction-quality crystals of the compounds in Table 1 were grown by vapor diffusion

Table 1. Crystallographic Data for $[Fe_4S_4(O\text{-}p\text{-}tol)_2(t\text{-}BuNC)_6]\cdot 1.5PhMe$ (**7**·1.5PhMe) and $[Fe_4S_4(SPh)_2(t\text{-}BuNC)_6]\cdot THF$ (**8**·THF)[a]

	7·1.5PhMe	**8**·THF
formula	$C_{54.5}H_{80}Fe_4N_6O_2S_4$	$C_{46}H_{72}Fe_4N_6OS_6$
fw	1203.04	1140.87
crystal system	monoclinic	monoclinic
space group	$P2_1/n$	$P2_1/n$
Z	4	4
a, Å	16.536(3)	21.900(6)
b, Å	12.133(2)	11.994(7)
c, Å	31.872(6)	22.865(7)
β, deg	95.62(4)	101.69(2)
V, Å^3	6364(2)	5882(4)
T, K	173	223
μ, cm^{-1}	10.65	12.20
R,[b] %	4.64	7.58
R_w,[c] %	4.92	7.71

[a] Radiation Mo Kα (λ = 0.710 69 Å). [b] $R = \sum||F_o| - |F_c||/\sum|F_o|$. [c] $R_w = \{\sum[w(|F_o| - |F_c|^2)]/\sum[w|F_o|^2]\}^{1/2}$.

(16) Christou, G.; Garner, C. D. *J. Chem. Soc., Dalton Trans.* **1979**, 1093.
(17) Dilworth, J. R.; Henderson, R. A.; Dahlstrom, P.; Nicholson, T.; Zubieta, J. A. *J. Chem. Soc., Dalton Trans.* **1987**, 529.

Table 2. Positional ($\times 10^4$) and Isotropic Thermal Parameters ($Å^2 \times 10^4$) for **7**·1.5PhMe

atom	x/a	y/b	z/c	U(iso)
Fe(1)	50079(9)	53781(13)	13892(4)	276(6)
Fe(2)	48361(9)	34501(13)	21732(4)	280(5)
Fe(3)	40017(9)	33289(13)	12633(5)	324(6)
Fe(4)	56621(9)	30010(13)	13989(5)	312(6)
S(1)	59059(17)	43893(24)	18718(8)	300(10)
S(2)	39628(16)	46488(24)	17615(8)	288(10)
S(3)	49777(18)	39365(24)	8673(8)	329(10)
S(4)	46708(17)	20069(24)	16629(8)	329(10)
O(1)	30240(45)	30069(68)	9402(23)	484(32)
O(2)	65033(48)	20671(64)	12771(23)	484(31)
N(1)	63211(61)	64224(79)	9197(28)	452(40)
N(2)	50134(59)	74985(83)	18630(29)	399(39)
N(3)	37522(62)	64310(84)	7738(29)	471(41)
N(4)	61741(59)	20671(84)	26262(27)	424(38)
N(5)	34164(62)	23648(82)	25419(29)	446(40)
N(6)	50457(58)	51378(82)	28598(29)	417(39)
C(1)	58399(74)	59801(95)	11066(34)	362(46)
C(2)	50341(67)	66133(99)	17094(32)	323(42)
C(3)	42356(76)	60359(93)	10170(34)	360(46)
C(4)	56423(71)	25944(93)	24560(31)	310(42)
C(5)	39674(66)	27996(91)	24014(32)	306(43)
C(6)	49512(62)	44961(105)	25878(34)	346(46)
C(111)	25436(79)	22002(118)	8549(38)	478(55)
C(112)	25443(78)	12431(118)	10937(46)	630(60)
C(113)	19953(94)	3736(136)	9774(54)	793(72)
C(114)	14654(102)	4078(161)	6316(62)	837(82)
C(115)	14330(86)	13491(176)	3925(44)	808(76)
C(116)	19562(85)	22396(142)	4969(40)	745(67)
C(117)	8698(92)	−5308(139)	5199(56)	1429(105)
C(211)	71583(74)	22231(102)	10870(35)	359(48)
C(212)	76025(68)	32230(111)	11218(34)	472(50)
C(213)	83009(73)	33590(121)	9130(39)	587(55)
C(214)	85896(72)	25526(126)	6656(37)	466(53)
C(215)	81612(76)	15518(120)	6251(35)	491(52)
C(216)	74630(73)	14014(106)	8368(34)	462(49)
C(217)	93517(73)	26868(128)	4367(40)	804(67)

of hexane into a toluene solution of **7** at room temperature and by layering hexane onto a THF solution of **8** at −20 °C. Single crystals were coated with Paratone-N oil and were attached to glass fibers. The crystals were transferred to a Nicolet P3v diffractometer and cooled in a nitrogen stream with a Siemens LT-2 cryostat operating at 173 K (**7**) or 223 K (**8**). Lattice parameters were obtained from a least-squares analysis of machine-centered reflections with $20° \leq 2\theta \leq 25°$. Crystal parameters are included in Table 1. Check reflections monitored every 100 reflections exhibited no significant decay over the course of the data collections. Lorentz and polarization corrections were applied with XDISK from the SHELXTL program package. An empirical absorption correction based on the observed variation in intensities of azimuthal (ψ) scans was applied to **8** using the program XEMP. Both compounds crystallize in the monoclinic system, and systematic absences are consistent with the space group $P2_1/n$.

Structure Solution and Refinement. The structures were solved by direct methods and were refined by full matrix least-squares and Fourier techniques. The asymmetric unit of **7** consists of one cluster, one toluene solvate molecule, and one-half toluene solvate molecule disordered across an inversion center. The asymmetric unit of **8** contains one cluster and one THF solvate molecule which displayed a great deal of thermal motion. The site occupancy factor of the THF molecule was refined and converged to 1. All non-hydrogen atoms in the clusters were refined anisotropically. In the final stages of refinement for both structures, hydrogen atoms were placed at idealized locations and were given uniform values of U_{iso}. In the last cycle of refinement, all parameters shifted by <1% of the esd of the parameter, and final difference Fourier maps showed no significant electron density. Final R factors are listed in Table 1 and atom positional parameters in Tables 2 and 3.[18]

Other Physical Measurements. All measurement were performed under anaerobic conditions. Absorption spectra were recorded on a Perkin-Elmer Lamba 4C spectrophotometer and IR spectra on a Nicolet IR/42 FT spectrophotometer. ^{1}H NMR spectra were obtained with use

Table 3. Positional ($\times 10^4$) and Isotropic Thermal Parameters ($Å^2 \times 10^4$) for **8**·THF

atom	x/a	y/b	z/c	U(iso)
Fe(1)	60179(9)	3328(17)	84305(9)	276(8)
Fe(2)	51241(9)	−15554(18)	74753(9)	310(8)
Fe(3)	46508(10)	6258(20)	78865(10)	432(9)
Fe(4)	54658(10)	7553(18)	71303(9)	361(9)
S(1)	60912(17)	−6514(33)	75498(16)	323(14)
S(2)	51443(17)	−7970(34)	84329(17)	343(15)
S(3)	54274(19)	18427(32)	79200(18)	387(16)
S(4)	45180(18)	−633(35)	69551(18)	445(16)
S(5)	37821(23)	12656(54)	81872(32)	1038(32)
S(6)	57251(23)	16826(41)	63459(19)	600(20)
N(1)	71304(57)	16939(114)	82729(58)	481(58)
N(2)	69377(64)	−11275(116)	92180(64)	576(63)
N(3)	57726(63)	14338(113)	95453(56)	516(60)
N(4)	51691(64)	−23171(114)	62325(59)	514(60)
N(5)	38394(63)	−25018(118)	74533(62)	558(62)
N(6)	57897(58)	−35074(104)	81301(56)	435(56)
C(1)	67114(75)	11584(131)	83451(61)	372(64)
C(2)	65519(70)	−6169(120)	88848(65)	342(60)
C(3)	58930(66)	10314(126)	91256(74)	394(65)
C(4)	51469(71)	−20442(129)	67105(77)	412(67)
C(5)	43444(86)	−21905(128)	74721(71)	490(71)
C(6)	55382(67)	−27509(117)	78858(68)	301(62)
C(111)	38850(85)	27007(201)	83521(104)	769(102)
C(112)	40899(101)	34442(260)	79527(96)	1049(126)
C(113)	41792(120)	45879(236)	80974(143)	1287(155)
C(114)	40577(171)	50689(319)	85975(151)	1714(220)
C(115)	38465(144)	43199(333)	89801(130)	1319(177)
C(116)	37648(94)	31639(268)	88696(122)	1044(138)
C(211)	52892(93)	29142(160)	64193(69)	538(80)
C(212)	46302(105)	29218(177)	62938(82)	747(98)
C(213)	43280(111)	39053(208)	63528(93)	856(108)
C(214)	46031(136)	48743(209)	65398(100)	935(124)
C(215)	52466(134)	48701(187)	66555(92)	912(115)
C(216)	55966(100)	39008(172)	65969(86)	777(96)

of a Bruker AM-400 spectrometer. Electrochemical measurements were carried out using standard PAR instrumentation, a Pt working electrode, an SCE reference electrode, and 0.1 M $(Bu_4N)(PF_6)$ supporting electrolyte in acetonitrile and dichloromethane solutions. Under the experimental conditions used here, $E_{1/2}(Fc^+/Fc) = +0.42$ V in dichloromethane and +0.39 V in acetonitrile. Mössbauer spectroscopic measurements were made as described;[19] isomer shifts are referenced to Fe metal at room temperature.

Results and Discussion

The following compounds are of primary interest in this work; of these, **2** and **5** have been prepared previously;[7] other clusters referred to are included in Figure 1

$[Fe_4S_4(LS_3)(t\text{-BuNC})_3]^{1-}$	**2**
$[Fe_4S_4Cl_2(MeNC)_6]$	**4**
$[Fe_4S_4Cl_2(t\text{-BuNC})_6]$	**5**
$[Fe_4S_4(O\text{-}p\text{-tol})_2(t\text{-BuNC})_6]$	**7**
$[Fe_4S_4(SPh)_2(t\text{-BuNC})_6]$	**8**
$[Fe_4S_4(S\text{-}p\text{-tol})_2(t\text{-BuNC})_6]$	**9**
$[Fe_4S_4(S\text{-}t\text{-Bu})_2(t\text{-BuNC})_6]$	**10**
$[Fe_4S_4(SEt)_2(t\text{-BuNC})_6]$	**11**

Preparation of Clusters. The clusters $[Fe_4S_4L_2(RNC)_6]$ have been prepared by the two routes in Figure 1. Clusters **4**−**6** were

(18) See paragraph at the end of this article for supplementary material available.

(19) Cen, W.; Lee, S. C.; Li, J.; MacDonnell, F. M.; Holm, R. H. *J. Am. Chem. Soc.* **1993**, *115*, 9515.

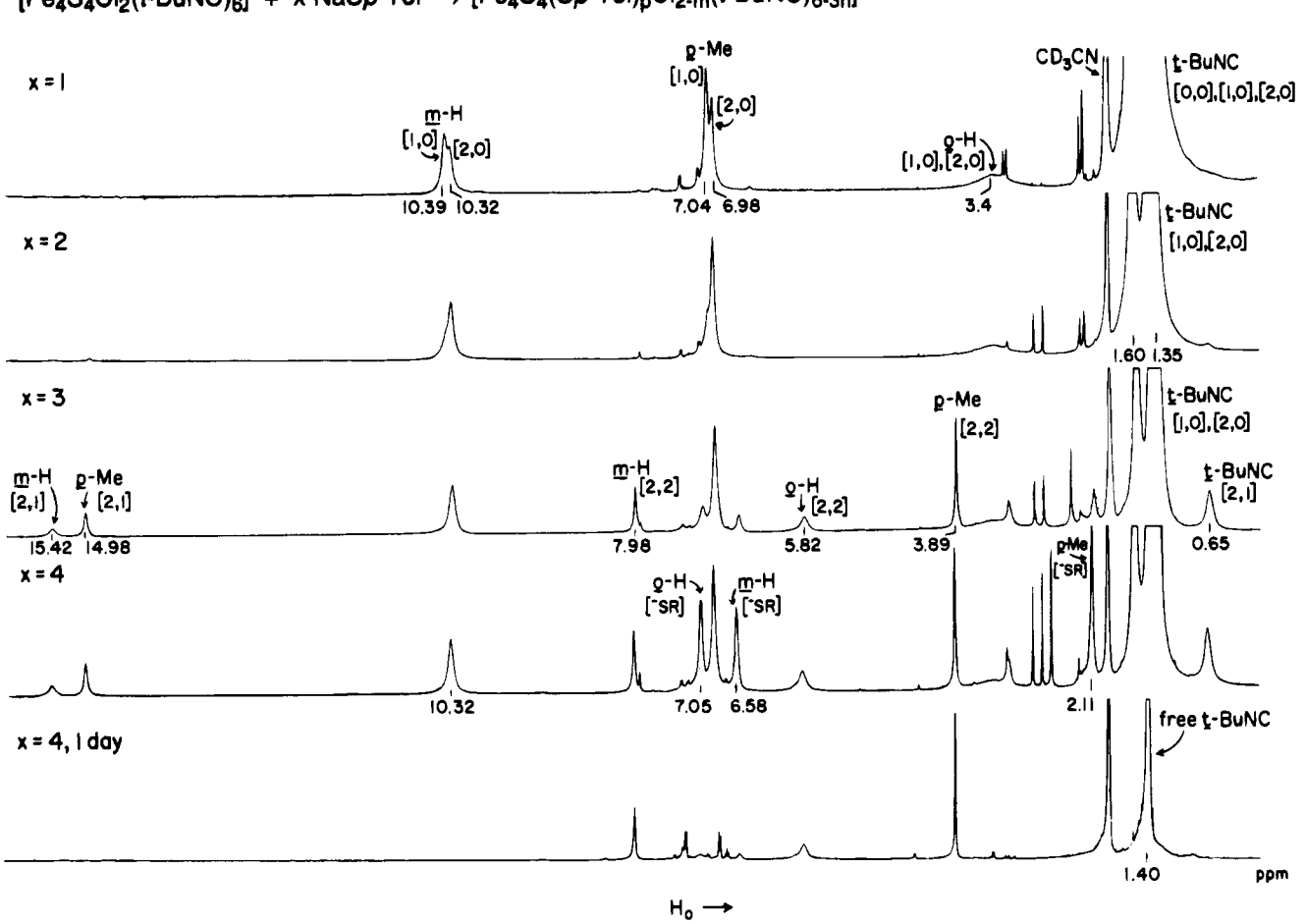

Figure 2. Stepwise substitution of cluster **5** with $x = 1-4$ equiv of *p*-toluenethiolate in CD_3CN solution at 298 K as monitored by ^1H NMR. Signal assignments of various species [*m*,*n*] are indicated. The first four spectra were recorded within 15 min of thiolate addition, and the last ($x = 4$) was recorded after 1 d. In each case, a solution of **5** was treated with an aliquot of a stock solution of Na(S-*p*-tol) in CD_3CN/CD_3OD (10:1 v/v).

obtained by reaction 2, in which THF solutions of $[Fe_4S_4X_4]^{2-}$ (X = Cl^-, Br^-) are refluxed with a 20-fold excess of the isonitrile. Product formation is assisted by precipitation of Et_4NX. Cluster **4** proved to be insufficiently soluble for further use. However, cluster **5**, which is freely soluble in low-polarity solvents, underwent facile chloride substitution in reaction 3 to afford the *p*-cresolate cluster **7** in 84% yield. Similarly, reaction 4 produced thiolate clusters **8**, **10**, and **11** in 45−66% yields. Reaction 5 provides an alternative synthesis of $[Fe_4S_4(SR)_2(RNC)_6]$ clusters and is based on our early observation that thiolate ligands of $[Fe_4S_4(SR)_4]^{2-}$ could be removed by acid treatment under controlled conditons with a high degree of retention of core structure.[8] Clusters **8**−**11** were prepared from the thiolate clusters **12**−**15** in 61−83% yields using salts of Et_3NH^+ in the presence of *ca.* 20-fold excess of *t*-BuNC in acetonitrile or THF solutions. As in the substitution of $[Fe_4S_4(SR)_4]^{2-}$ by $R'S^-$,[20] the likely course of events in the overall reaction (5) is protonation of bound thiolate, dissociation

$$[Fe_4S_4(SR)_4]^{2-} + 2Et_3NH^+ + 6t\text{-BuNC} \rightarrow [Fe_4S_4(SR)_2(t\text{-BuNC})_6] + 2Et_3N + 2RSH \quad (5)$$

of thiol, and binding of isonitrile at the unsaturated iron site. As will be seen, this process must involve a spin state change at the site and a significant dimensional change of the $[Fe_4S_4]^{2+}$ core.

(20) Henderson, R. A.; Oglieve, K. E. *J. Chem. Soc., Dalton Trans.* **1993**, 1467.

Ligand Substitution Reactions. In order to probe the relative stabilities of certain substituted clusters, the reaction system in Figure 2 was monitored by ^1H NMR in acetonitrile solution. Typically, a solution of **5** of known concentration was treated with an aliquot of a stock solution of Na(S-*p*-tol) in CD_3CN/CD_3OD (10:1 v/v), the reaction mixture was immediately shaken, and the spectrum was recorded after 15 min. Addition of $x \geq 1$ equiv of thiolate resulted in a color change from purple to brown. The symbols [*m*,*n*] refer to the product clusters, where *m* and *n* are the number of chloride and tris(isonitrile) binding sites substituted, respectively.

At $x = 1$ equiv of thiolate, approximately equal amounts of the clusters [0,0] = **5**, [1,0] = $[Fe_4S_4Cl(S\text{-}p\text{-tol})(t\text{-BuNC})_6]$, and [2,0] = **9** are present. With the addition of $x = 2$ equiv, [2,0] is the major product, with a much smaller amount of [1,0] and a trace of [2,1] = $[Fe_4S_4(S\text{-}p\text{-tol})_3(t\text{-BuNC})_3]^-$ formed. This is the basis of reactions 3 and 4. When conducted on a preparative scale, these reactions employed a small excess of the substituting ligand and a 10-fold excess of isonitrile in order to diminish or eliminate substitution at the tris(isonitrile) sites. Solutions of **5** in acetonitrile show a signal at 1.41 ppm corresponding to unbound isonitrile, but overlap with bound isonitrile resonances prevented accurate integration. All other clusters, including **2**, also dissociate small amounts of isonitrile. Free and bound ligand are in slow exchange; all [2:2] site-differentiated clusters show two methyl or *tert*-butyl resonances in a 2:1 intensity ratio (not shown), consistent with the C_2 symmetry found in the solid state (vide infra). On the basis of ^1H NMR spectra, clusters

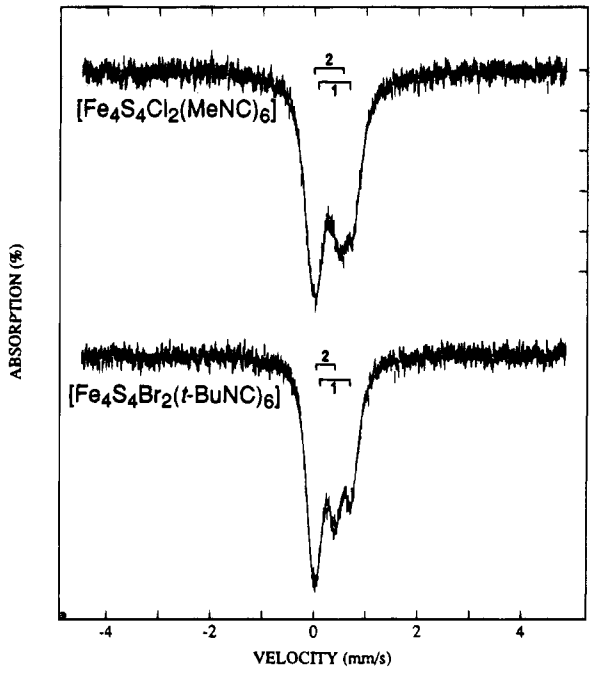

Figure 3. Zero-field ^{57}Fe Mössbauer spectra of clusters **4** and **6** at 77 K. Quadrupole doublets 1 and 2 are due to the high-spin Iron(III) halide and low-spin tris(isonitrile)iron(II) sites, respectively.

4−**13** do not undergo any detectable extent of disproportionation in acetonitrile, dichloromethane, or THF solutions.

In reactions with $x = 3$ and 4 equiv substitution at the tris(isonitrile) sites was markedly slower than at a Fe−Cl site. At $x = 3$ equiv, the dominant species are [2,0], [2,2] = **13**, and [2,1] in *ca.* 3:2:1 ratio; a small amount of unreacted thiolate is also evident. The identification of the latter species, which is a [1:3] site-differentiated cluster, follows from the properties of **2** whose $S = 2$ ground state affords large isotropic shifts of the coordinated benzenethiolate ligands.[21] The coexistence of the three clusters indicates the disproportionation equilibrium (6) and probable difficulty in isolating a pure sample of the [2,1] cluster. Tris(isonitrile) cluster **2** is constrained from an analogous reaction.

$$2[Fe_4S_4(S\text{-}p\text{-}tol)_3(t\text{-}BuNC)_3]^- \rightleftharpoons [Fe_4S_4(S\text{-}p\text{-}tol)_4]^{2-} + [Fe_4S_4(S\text{-}p\text{-}tol)_2(t\text{-}BuNC)_6] \quad (6)$$

At $x = 4$ equiv after 15 min, the species [2,0], [2,2], and [2,1] are generated in *ca.* 1:2:2 ratio, but with substantial thiolate unreacted. After 1 d, thiolate cluster **13** is the sole product. The reactions were repeated in homogeneous systems using (Et_4N)(S-*p*-tol) as the thiolate source; the results correlated well with those just described.

Mössbauer Spectra and Electronic Features. The spectra of clusters **4**−**11** consist of two partially resolved doublets; those of **4** and **6** are shown in Figure 3. All spectra were fitted satisfactorily as two doublets with a constrained 1:1 intensity ratio using parameters in Table 4. For site 1, the isomer shift (δ) and quadrupole splitting (ΔE_Q) define the ranges 0.29−0.41 and 0.39−0.68 mm/s, respectively. These correspond very well to those expected for high-spin Fe(III) in a mainly or wholly anionic sulfur environment. For example, the data for the Et_4N^+ salts of $[Fe_2S_2(OPh)_4]^{2-}$ ($\delta = 0.37$ mm/s, $\Delta E_Q = 0.32$ mm/s)[22] and $[Fe_2S_2(SPh)_4]^{2-}$ ($\delta = 0.29$ mm/s, $\Delta E_Q = 0.32$ mm/s)[23] are consistent with this assignment. When the isomer shifts are used in our empirical correlation with oxidation state s of Fe in a tetrahedral sulfur environment ($\delta = 1.36 - 0.36s$),[19] $s = 2.8$−3.0 for clusters **8**−**11**, providing further support for the Fe(III) formulation. The order of decrease in isomer shifts, $Cl^- \gtrsim RO^- > RS^-$, is that commonly found in Fe_2S_2 and Fe_4S_4 clusters.[22-26]

Table 4. Mössbauer Parameters of the Clusters $[Fe_4S_4L_2(RNC)_6]^a$

L	site	δ,[b] mm/s	ΔE_Q, mm/s
Cl^- (**4**)	1	0.41	0.68
	2[c]	0.20	0.55
Cl^- (**5**)[d]	1	0.41	0.60
	2	0.19	0.45
Br^- (**6**)	1	0.40	0.64
	2	0.18	0.46
p-$MeC_6H_4O^-$ (**7**)	1	0.37	0.65
	2	0.17	0.48
PhS^- (**8**)	1	0.34	0.39
	2	0.16	0.43
p-$MeC_6H_4S^-$ (**9**)	1	0.33	0.44
	2	0.18	0.48
t-BuS^- (**10**)	1	0.35	0.54
	2	0.17	0.49
EtS^- (**11**)	1	0.29	0.67
	2	0.19	0.46
$[Fe_4S_4(LS_3)(t\text{-}BuNC)_3]^-$ (**2**)[d]	1[e]	0.42	1.10
	2	0.20	0.50

[a] All measurements at 77 K. R = *t*-Bu except for **4**. [b] Relative to Fe metal at room temperature. [c] Site 2 is low-spin Fe(II). [d] Reference 7. [e] Mean values of three sites.

The magnetic properties of the site 1 $[Fe_2S_2]^{2+}$ core fragment conform to expectations for two antiferromagnetically coupled Fe(III) sites. The magnetic moments per Fe atom are $\mu_{Fe} = 1.41$ and 1.36 μ_B for **5** and **7**, respectively, in dichloromethane solution at room temperature. These compare favorably with $\mu_{Fe} = 1.4$−$1.9\mu_B$ for $[Fe_2S_2L_4]^{2-}$ (L = Cl^-, PhS^-, PhO^-, *p*-$tolO^-$);[22-24] several of these species have been shown to be antiferromagnetic by measurements over a suitable temperature range in the solid state.[23] The isotropically shifted resonances of the species in Figure 2 arise from the paramagnetism of this fragment.

For site 2, $\delta = 0.16$−0.20 mm/s and $\Delta E_Q = 0.43$−0.55 mm/s. These values are consistent with low-spin Fe(II) and vary only slightly over the set **4**−**11**. They correlate very well with those for the unique subsite of cluster **2**, whose magnetically perturbed spectrum has shown the existence of an effectively diamagnetic subsite with the parameters in Table 4. Consequently, site 2 is the low-spin $Fe^{II}S_3(RNC)_3$ unit.

Cluster Structures. The structures of solvated forms of **7** and **8** have been determined by X-ray methods and are set out in Figure 4. While there is no imposed symmetry, both clusters closely approach C_2 symmetry, as indicated by the consecutive pairwise listing of symmetry-related angles and distances in Table 5. The $[Fe_4S_4]^{2+}$ cores are built up by edge-shared nonplanar Fe_2S_2 rhombs which are the core faces.

Core structures depart markedly from the 4 short + 8 long Fe−S bond length pattern of standard clusters such as

(21) Chemical shift comparison (ppm), **2**/[2:1]: 0.38/0.66 (*t*-Bu), 14.94/14.98 (6-Me/*p*-Me), 16.52/15.42 (5-H/*m*-H).

(22) Cleland, W. E., Jr.; Averill, B. A. *Inorg. Chem.* **1984**, *23*, 4192.
(23) Gillum, W. O.; Frankel, R. B.; Foner, S.; Holm, R. H. *Inorg. Chem.* **1976**, *15*, 1095.
(24) Salifoglou, A.; Simopoulos, A.; Kostikas, A.; Dunham, W. R.; Kanatzidis, M. G.; Coucouvanis, D. *Inorg. Chem.* **1988**, *27*, 3394.
(25) Cleland, W. E.; Holtman, D. A.; Sabat, M.; Ibers, J. A.; DeFotis, G. C.; Averill, B. A. *J. Am. Chem. Soc.* **1983**, *105*, 6021.
(26) Kanatzidis, M. G.; Baenziger, N. C.; Coucouvanis, D.; Simopoulos, A.; Kostikas, A. *J. Am. Chem. Soc.* **1984**, *106*, 4500.

$[Fe_4S_4(O\text{-}C_6H_4\text{-}CH_3)_2(t\text{-}BuNC)_6]$

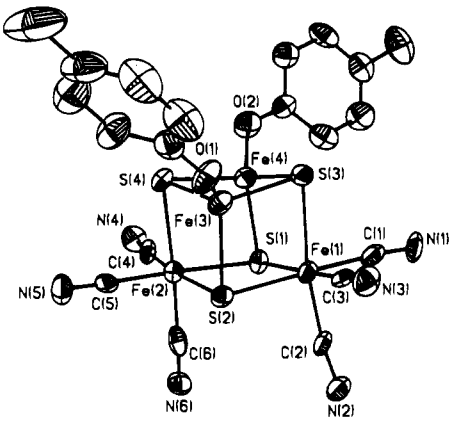

$[Fe_4S_4(S\text{-}C_6H_5)_2(t\text{-}BuNC)_6]$

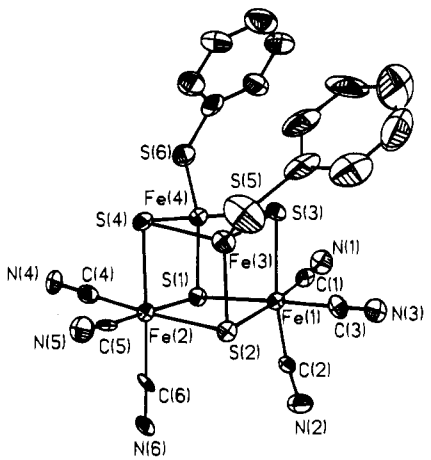

Figure 4. Structures of clusters **7** (top) and **8** (bottom), showing 50% (**7**) and 35% (**8**) probability ellipsoids and the atom-labeling schemes. For clarity, the *tert*-butyl groups of the isonitrile ligands have been omitted.

$[Fe_4S_4(OPh)_4]^{2-}$[25] and $[Fe_4S_4(SPh)_4]^{2-}$.[27] Instead, the Fe–S distances divide into 6 short at tetrahedral sites Fe(3,4) with mean values of 2.263(7) Å (**7**) and 2.25(1) Å (**8**) and 6 long at the six-coordinate sites Fe(1,2) with mean values of 2.38(2) Å (**7**) and 2.37(2) Å (**8**). Coincident with this array of distances are Fe–Fe separations which clearly distinguish the core faces. Thus, in the Fe(3,4)S(3,4) faces, which are perpendicular to the idealized C_2 axes, the Fe–Fe distances are 2.766(2) Å (**7**) and 2.730(4) Å (**8**). These compare fairly well with the corresponding distances of 2.75(2) and 2.691(1) Å in $[Fe_2S_2(O\text{-}p\text{-}tol)_4]^{2-}$ [24] and $[Fe_2S_2(S\text{-}p\text{-}tol)_4]^{2-}$,[28] respectively. In addition, the mean terminal distances at these sites, 1.868 Å (**7**) and 2.281 Å (**8**), are in good agreement with those of $[Fe_2S_2(O\text{-}p\text{-}tol)_4]^{2-}$ (1.87(2) Å) and $[Fe_2S_2(S\text{-}p\text{-}tol)_4]^{2-}$ (2.312 Å), respectively. These comparisons provide additional evidence that the tetrahedral sites contain Fe(III).

Core faces parallel to the idealized C_2 axes exhibit Fe–Fe distances somewhat larger than that of the foregoing perpendicular face, the ranges being 2.986(2)–3.091(2) Å for **7** and 3.017(3)–3.033(4) Å for **8**. In remaining perpendicular faces, Fe(1,2)S(1,2), the Fe–Fe separations are maximal and essentially identical, 3.455(2) Å for **7** and 3.465(3) Å for **8**. These separations, together with the low-spin nature of Fe(1,2), result in isolation of the opposite face as an antiferromagnetically coupled $[Fe^{III}_2S_2]^{2+}$ fragment analogous to cores of various binuclear clusters of the type $[Fe_2S_2L_4]^{2-}$.[22-24,28] In Fe_4S_4 clusters, the extreme case of site isolation is found with $[Fe_4S_4(CO)_{12}]$, where the low-spin sites are separated by 3.47 Å.[29] The core structures of clusters **5**, **7**, and **8** are nearly congruent; these three cases now define the structural motif for $[Fe_4S_4]^{2+}$ clusters with two six-coordinate low-spin Fe(II) and two tetrahedral high-spin Fe(III) sites. A structural analysis of **5**, more detailed than that given here for the other two clusters, has been presented elsewhere.[7]

Table 5. Selected Interatomic Distances (Å) and Angles (deg) for **7**·1.5PhMe and **8**·THF

	7·1.5PhMe	**8**·THF
	Fe_4S_4 Core	
Fe(1)–S(3)	2.411(3)	2.388(4)
Fe(2)–S(4)	2.387(3)	2.396(5)
Fe(3)–S(2)	2.261(3)	2.257(5)
Fe(4)–S(1)	2.270(3)	2.261(4)
Fe(1)–S(2)	2.362(3)	2.345(5)
Fe(2)–S(1)	2.384(3)	2.355(4)
Fe(1)–S(1)	2.359(3)	2.368(5)
Fe(2)–S(2)	2.356(3)	2.363(5)
Fe(3)–S(3)	2.267(3)	2.231(5)
Fe(4)–S(4)	2.263(3)	2.258(5)
Fe(3)–S(4)	2.268(3)	2.248(5)
Fe(4)–S(3)	2.250(3)	2.243(5)
Fe(1)–Fe(3)	2.997(2)	3.021(3)
Fe(2)–Fe(4)	2.986(2)	3.018(4)
Fe(1)–Fe(4)	3.079(2)	3.017(3)
Fe(2)–Fe(3)	3.091(2)	3.033(4)
Fe(1)–Fe(2)	3.455(2)	3.465(3)
Fe(3)–Fe(4)	2.776(2)	2.730(4)
S(1)–Fe(1)–S(2)	85.8(1)	84.8(2)
S(1)–Fe(2)–S(2)	85.4(1)	84.7(1)
S(1)–Fe(1)–S(3)	92.9(1)	94.9(2)
S(2)–Fe(2)–S(4)	92.9(1)	94.4(2)
S(2)–Fe(1)–S(3)	96.2(1)	94.5(2)
S(1)–Fe(2)–S(4)	96.7(1)	95.3(2)
S(3)–Fe(3)–S(4)	102.0(1)	103.0(2)
S(3)–Fe(4)–S(4)	102.7(1)	102.3(2)
S(2)–Fe(3)–S(3)	103.4(1)	101.5(2)
S(1)–Fe(4)–S(4)	103.7(1)	101.9(2)
S(2)–Fe(3)–S(4)	98.8(1)	101.7(2)
S(1)–Fe(4)–S(3)	99.7(1)	102.2(2)
Fe(1)–S(1)–Fe(2)	93.5(1)	94.4(2)
Fe(1)–S(2)–Fe(2)	94.2(1)	94.7(2)
Fe(1)–S(2)–Fe(3)	80.8(1)	82.0(2)
Fe(2)–S(1)–Fe(4)	79.8(1)	81.6(1)
Fe(2)–S(2)–Fe(3)	84.0(1)	82.0(1)
Fe(1)–S(1)–Fe(4)	83.4(1)	81.3(1)
Fe(2)–S(4)–Fe(4)	79.8(1)	80.8(1)
Fe(1)–S(3)–Fe(3)	79.6(1)	81.6(2)
Fe(2)–S(4)–Fe(3)	83.2(1)	81.5(1)
Fe(1)–S(3)–Fe(4)	82.6(1)	81.2(2)
Fe(3)–S(3)–Fe(4)	75.5(1)	75.2(1)
Fe(3)–S(4)–Fe(4)	75.3(1)	74.6(1)
	Terminal Ligation	
Fe(3)–O(1)/S(5)	1.871(7)	2.283(7)
Fe(4)–O(2)/S(6)	1.864(8)	2.278(5)
O(1)/S(5)–Fe(3)–S(2–4) range	112.7(3)–120.6(3)	115.0(2)–116.9(2)
O(2)/S(6)–Fe(4)–S(1,3,4) range	109.6(3)–120.1(3)	114.0(2)–118.2(2)
Fe(1,2)–C(1–6) range	1.81(1)–1.87(1)	1.80(1)–1.87(2)
mean of 6	1.84(2)	1.85(2)
Fe(1,2)–C–N range	170(1)–179(1)	172(1)–179(1)
C–Fe(1,2)–C range	88.3(5)–96.8(5)	87.1(7)–97.4(7)

(27) (a) Que, L., Jr.; Bobrik, M. A.; Ibers, J. A.; Holm, R. H. *J. Am. Chem. Soc.* **1974**, *96*, 4168. (b) Excoffon, P.; Laugier, J.; Lamotte, B. *Inorg. Chem.* **1991**, *30*, 3075.

(28) Mayerle, J. J.; Denmark, S. E.; DePamphilis, B. V.; Ibers, J. A.; Holm, R. H. *J. Am. Chem. Soc.* **1975**, *97*, 1032.

(29) Nelson, L. L.; Lo, F. Y.-K.; Rae, A. D.; Dahl, L. F. *J. Organomet. Chem.* **1982**, *225*, 309.

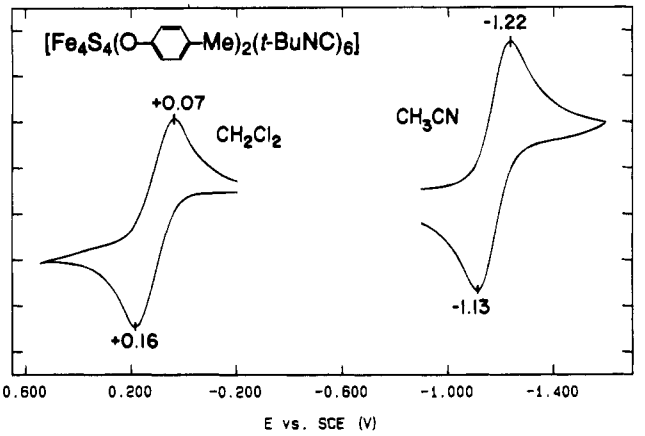

Figure 5. Partial cyclic voltammograms (50 mV/s) of cluster **7** in acetonitrile and dichloromethane showing reversible reduction and oxidation, respectively. Peak potentials vs SCE are indicated.

Table 6. Redox Potentials of the Clusters $[Fe_4S_4L_2(t\text{-BuNC})_6]$

L	$E_{1/2}$[a] V (redn,[b] MeCN)	$E_{1/2}$,[a] V (oxdn,[c] CH_2Cl_2)
Cl^- (**5**)	−0.95	+0.23
Br^- (**6**)	−0.89	+0.25
p-$MeC_6H_4O^-$ (**7**)	−1.18	+0.12
PhS^- (**8**)	−1.11	+0.03[d]
p-$MeC_6H_4S^-$ (**9**)	−1.13	0.00[d]
t-BuS^- (**10**)	−1.33	−0.10[d]
EtS^- (**11**)	−1.28	~0[e]

[a] $E_{1/2} = (E_{pc} + E_{pa})/2$; vs SCE. [b] $\Delta E_p = 80-90$ mV. [c] $\Delta E_p = 90-140$ mV. [d] Quasi-reversible. [e] Irreversible.

Redox Reactions. The behavior of clusters **5**−**11** has been examined in acetonitrile and dichloromethane solutions by cyclic voltammetry. A typical voltammogram is shown in Figure 5; potentials are listed in Table 6. In general, the clusters show the three-membered electron transfer series (7) but not in the same solvent. Chemically reversible reductions occur in acetonitrile and oxidations in dichloromethane ($i_{pa}/i_{pc} \sim 1$). Oxidations in acetonitrile and reductions in dichloromethane are poorly developed and for the most part irreversible. The ligand dependence of potentials for reduction is in the order established for Fe_2S_2 and Fe_4S_4 clusters[13,22-25,28,30] and, therefore, is consistent with reduction of the $[Fe_2S_2]^{2+}$ fragment. Oxidation reactions presumably involve the low-spin Fe(II) sites, there being no evidence in Fe−S clusters of any kind for the stabilization of Fe(IV). If so, the ligands at sites *ca.* 3 Å removed from the locus of oxidation exhibit a substantial (and unexpected) influence on potentials. Addition of a 15-fold excess of the isonitrile rendered the oxidations irreversible.

$$[Fe_4S_4L_2(t\text{-BuNC})_6]^+ \rightleftarrows [Fe_4S_4L_2(t\text{-BuNC})_6] \rightleftarrows [Fe_4S_4L_2(t\text{-BuNC})_6]^- \quad (7)$$

Summary. The following are the principal results and conclusions of this investigation.

1. Clusters of the type $[Fe_4S_4X_2(RNC)_6]$ can be prepared in good yield by direct reaction of the isonitrile with the halide cluster $[Fe_4S_4X_4]^{2-}$. Substitution reactions proceed initially at the halide sites and afford $[Fe_4S_4L_2(RNC)_6]$ (L = RO^-, RS^-). Alternatively, thiolate clusters can be prepared in the reaction system $[Fe_4S_4(SR)_4]^{2-}/Et_3NH^+/RNC$ (excess) in which the probable pathway involves protonation of bound thiolate, thiol dissociation, and isonitrile binding. Treatment of $[Fe_4S_4(SR)_2(RNC)_6]$ with additional thiolate results in substitution at the tris(isonitrile) sites and eventual formation of $[Fe_4S_4(SR)_4]^{2-}$.

2. Mössbauer spectra of eight clusters of the type $[Fe_4S_4L_2(t\text{-BuNC})_6]$ indicate the presence of two high-spin tetrahedral Fe(III) sites and two low-spin Fe(II) sites.

3. The X-ray structures of the clusters $[Fe_4S_4L_2(t\text{-BuNC})_6]$ (L = Cl^-,[7] p-$tolO^-$, PhS^-) reveal imposed or idealized C_2 core symmetry, are consistent with the results of (2), and demonstrate the presence of six-coordinate low-spin sites at nonbonding distances from each other and from the two tetrahedral sites. The latter are implicated in an $[Fe_2S_2]^{2+}$ fragment very similar to the cores of the antiferromagnetically coupled clusters $[Fe_2S_2L_4]^{2-}$. The essential congruency of the cores of *three* clusters defines the structural motif of $[Fe_4S_4]^{2+}$ with two tetrahedral Fe(III) and two low-spin six-coordinate Fe(II) sites.

4. The clusters $[Fe_4S_4L_2(RNC)_6]$ represent the most extensively developed class of [2:2] site-differentiated Fe_4S_4 clusters. Because of their substantial utility,[1-7,9,12] interest in site-differentiated clusters is growing; evidence for two new types of [1:3] clusters was recently presented.[31,32] One current intention is to utilize [2:2] clusters as precursors in cluster-bridging reactions involving displacement of labile L ligands followed by substitution of isonitrile ligands; such reactions are precedented in the system of Figure 2. Research addressing this possibility is underway.

Acknowledgment. This research was supported by NIH Grant 28856. X-ray equipment was obtained through NIH Grant 1 S10 RR 02247. We thank Dr. L. Cai and M. J. Scott for experimental assistance and useful discussions.

Supplementary Material Available: X-ray crystallographic data for the compounds in Table 1, including tables of intensity collection and structure refinement parameters, positional and thermal parameters, bond distances and angles, and calculated hydrogen atom positions (19 pages). Ordering information is given on any current masthead page.

(30) DePamphilis, B. V.; Averill, B. A.; Herskovitz, T.; Que, L., Jr.; Holm, R. H. *J. Am. Chem. Soc.* **1974**, *96*, 4159.

(31) (a) Martens, C. F.; Blonk, H. L.; Bongers, T.; van der Linden, J. G. M.; Beurskens, G.; Beurskens, P. T.; Smits, J. M. M.; Nolte, R. J. M. *J. Chem. Soc., Chem. Commun.* **1991**, 1623. (b) van Strijdonck, G. P. F.; van Haare, J. A. E. H.; van der Linden, J. G. M.; Steggerda, J. J.; Nolte, J. J. M. *Inorg. Chem.* **1994**, *33*, 999.

(32) Evans, D. J.; Garcia, G.; Leigh, G. J.; Newton, M. S.; Santana, M. D. *J. Chem. Soc., Dalton Trans.* **1992**, 3229.